Combining antibiotics with antivirulence compounds is effective and can reverse selection for antibiotic resistance in *Pseudomonas aeruginosa*

Chiara Rezzoagli[1,2], Martina Archetti[1,2], Michael Baumgartner[3], Rolf Kümmerli[1,2*]

[1]Department of Quantitative Biomedicine, University of Zurich, Zurich, Switzerland

[2]Department of Plant and Microbial Biology, University of Zurich, Zurich, Switzerland

[3] Institute for Integrative Biology, Department of Environmental Systems Science, ETH Zurich, Zurich, Switzerland

Short title: Antibiotic-antivirulence combination therapy against bacterial pathogens

Corresponding author: Rolf Kümmerli, Department of Quantitative Biomedicine, University of Zurich, Winterthurerstrasse 190, 8057 Zurich, Switzerland.

Email: rolf.kuemmerli@uzh.ch / Phone: +41 44 635 48 01.

Abstract

Antibiotics are losing efficacy due to the rapid evolution and spread of resistance. Treatments targeting bacterial virulence factors have been considered as alternatives because they target virulence instead of pathogen viability, and should therefore exert weaker selection for resistance than conventional antibiotics. However, antivirulence treatments rarely clear infections, which compromises their clinical applications. Here, we explore the potential of combining antivirulence drugs with antibiotics against the opportunistic human pathogen *Pseudomonas aeruginosa*. We combined two antivirulence compounds (gallium, a siderophore-quencher, and furanone C-30, a quorum sensing-inhibitor) together with four clinically relevant antibiotics (ciprofloxacin, colistin, meropenem, tobramycin) in 9x9 drug concentration matrices. We found that drug-interaction patterns were concentration dependent, with clinically interesting levels of synergies occurring at intermediate drug concentrations for certain drug pairs. We then tested whether antivirulence compounds are potent adjuvants, especially when treating antibiotic resistant clones. We found that the addition of antivirulence compounds to antibiotics could restore growth inhibition for most antibiotic resistant clones, and even reverse selection for resistance in three drug combination cases. Molecular analyses suggest that selection reversal occurs when resistance mechanisms involve restoration of protein synthesis, but not when efflux pumps are upregulated. Altogether, our work provides a first systematic analysis of antivirulence-antibiotic combinatorial treatments and suggests that such combinations have a high potential to be both effective in treating infections and in limiting the spread of antibiotic resistance.

Introduction

Scientists together with the World Health Organization (WHO) forecast that the rapid evolution and spread of antibiotic resistant bacteria will lead to a world-wide medical crisis [1–3]. Already today, the effective treatment of an increasing number of infectious diseases has become difficult in many cases [4,5]. To avert the crisis, novel innovative approaches that are both effective against pathogens and robust to the emergence and spread of resistance are urgently needed [6,7]. One such approach involves the use of compounds that disarm rather than kill bacteria. These so-called 'antivirulence' treatments should exert weaker selection for resistance compared to classical antibiotics because they simply disable virulence factors but are not supposed to affect pathogen viability [8–10]. However, a downside of antivirulence approaches is that the infection will not necessarily be cleared. This could be particularly problematic for immuno-compromised patients (AIDS, cancer, cystic fibrosis and intensive-care unit patients), whose immune system is conceivably too weak to clear even disarmed pathogens.

One way to circumvent this problem is to combine antivirulence compounds with antibiotics to benefit from both virulence suppression and effective pathogen removal [6,11]. While a few studies have already considered such combinatorial treatments [12–18], we currently have no comprehensive understanding of how different types of antibiotics and antivirulence drugs interact, whether interactions are predominantly synergistic or antagonistic, and how combinatorial treatments affect the spread of antibiotic resistance. Here, we tackle these open issues by combining four different classes of antibiotics with two antivirulence compounds, in 9x9 drug concentration

matrixes, as treatments against the opportunistic human pathogen *Pseudomonas aeruginosa*.

P. aeruginosa is one of the ESKAPE pathogens with multi-drug resistant strains spreading worldwide and infections becoming increasingly difficult to treat [19,20]. In addition to its clinical relevance, *P. aeruginosa* has become a model system for antivirulence research. Several antivirulence compounds targeting either the species' quorum sensing (QS) [21–23] or siderophore-mediated iron uptake systems [24–27] have been proposed. While QS is a cell-to-cell communication system that controls the expression of multiple virulence factors including exo-proteases, biosurfactants and toxins, siderophores are secondary metabolites important for the scavenging of iron from host tissue. For our experiments, we chose antivirulence compounds that target these two different virulence mechanisms: furanone C-30, an inhibitor of the LasR QS-system [12,21], and gallium, targeting the iron-scavenging pyoverdine and iron-metabolism [24,26,28–32].

Furanone C-30 is a synthetic, brominated furanone, which includes the same lactone ring present in the acylhomoserine lactones (AHL) QS molecules of *P. aeruginosa* [33]. As a consequence, it can disrupt QS-based communication by antagonistically competing with the AHLs molecules for binding to the main QS (LasR) receptor [34]. Gallium is an iron mimic whose ionic radius and coordination chemistry is comparable to ferric iron, although its redox properties are different. Specifically, gallium cannot be reduced and thereby irreversibly binds to siderophores and hinders siderophore-mediated iron uptake [24,26].

We combined the two antivirulence compounds with four clinically relevant antibiotics (ciprofloxacin, colistin, meropenem, and tobramycin), which are widely used against *P. aeruginosa* [35]. In a first step, we measured treatment effects on bacterial growth and virulence factor production for all eight drug combinations for 81 concentration combinations each. In a second step, we applied the Bliss independence model to calculate the degree of synergy or antagonism to obtain comprehensive interaction maps for all combinations both for growth and virulence factor production. Next, we selected for antibiotic resistant clones and tested whether the addition of antivirulence compounds as adjuvants can re-potentiate antibiotics and reverse selection for resistance. Finally, we sequenced the genomes of the evolved antibiotic resistant clones to examine the genetic basis that drive the observed patterns of cross-resistance and resistance reversal.

Results

PAO1 dose-response curves to antibiotics and antivirulence compounds

In a first experiment, we determined the dose-response curve of PAO1 to each of the four antibiotics (Figure 1) and the two anti-virulence compounds (Figure 2) in our experimental media. We found that the dose-response curves for antibiotics followed sigmoid functions (Figure 1), characterised by (i) a low antibiotic concentration range that did not inhibit bacterial growth, (ii) an intermediate antibiotic concentration range that significantly reduced bacterial growth, and (iii) a high antibiotic concentration range that completely stalled bacterial growth.

Similar dose-response curves were obtained for gallium (quenching pyoverdine) and furanone C-30 (inhibiting protease production) in the respective media where the two

115 virulence factors are important for growth (Figure 2). Crucially, the dose-response
116 curves shifted to the right (extending phase (i)) when we repeated the experiment in
117 media, where the virulence factors are not needed for growth (i.e. iron-rich media for
118 pyoverdine, and protein digest media for proteases). This shows that there is a
119 window of concentrations where growth inhibition is caused by virulence factor
120 quenching alone. Conversely, high concentrations of antivirulence compounds seem
121 to have additional off-target effects curbing growth.
122
123 **Interaction maps of antibiotic-antivirulence drug combinations**
124 *General patterns*. From the dose-response curves, we chose 9 concentrations for
125 each drug to cover the entire trajectory, from no to intermediate to high growth
126 inhibition. We then combined antibiotics with antivirulence compounds in a 9x9
127 concentration matrix and measured the dose-response curve for every single drug
128 combination for both growth and virulence factor production (Figure 3). At the
129 qualitative level, independent drug effects would cause a symmetrical downshift of
130 the dose-response curve with higher antivirulence compound concentrations
131 supplemented. We indeed noticed symmetrical downshifts for many dose-response
132 curves (Figure 3), but there were also clear cases of non-symmetrical shifts,
133 indicating synergy or antagonism between drugs. When using the Bliss model to
134 quantify these effects, we found patterns of synergy and antagonism for both growth
135 and virulence factor inhibition across the concentration matrices for all drug
136 combinations (Figure 4).
137
138 *Gallium-antibiotic combinations*. Gallium combined with ciprofloxacin or colistin had
139 mostly independent effects on bacterial growth (i.e. weak or no synergy/antagonism)

140 (Figures 4A+B). With regard to the inhibition of pyoverdine production, both drug
141 combinations showed a tendency towards stronger synergy at intermediate drug
142 concentrations (Figure 4E+F). For gallium-meropenem combinations, we observed
143 mostly independent interactions for growth and pyoverdine inhibition, with small
144 hotspots of antagonism (for growth) and synergy (for siderophore inhibition) existing
145 at intermediate drug concentrations (Figure 4C+G). Finally, for gallium-tobramycin
146 combinations there were relatively strong synergistic interactions for both growth
147 (Figure 4D) and pyoverdine inhibition (Figure 4H) at intermediate drug
148 concentrations.
149
150 *Furanone-antibiotic combinations*. For furanone-ciprofloxacin combinations, we found
151 relatively strong antagonistic interactions with regard to growth inhibition (Figure 4I),
152 whereas effects on protease inhibition were mostly independent (Figure 4M). In
153 contrast, for furanone-colistin combinations we observed strong synergistic drug
154 interactions especially for intermediate and higher concentrations of the antivirulence
155 compound for growth and protease inhibition (Figure 4J+N). Furanone-meropenem,
156 on the other hand, interacted mostly antagonistically with regard to growth and
157 protease inhibition (Figure 4K+O). Conversely, for furanone-tobramycin combinations
158 there were pervasive patterns of synergy across the entire drug combination range
159 for growth and virulence factor inhibition (Figure 4L+P).
160
161 *Do the degrees of synergy for growth and virulence factor inhibition correlate?* As the
162 combinatorial treatments affect both growth and virulence factor production, we
163 examined whether the degrees of synergy correlate between the two traits
164 (Supplementary Figure S1). For gallium-antibiotic combinations, we found no

165 correlations for ciprofloxacin and meropenem, but positive associations for colistin
166 and tobramycin (Pearson correlation coefficient; ciprofloxacin: $r = 0.09$, $t_{79} = 0.85$, $p =$
167 0.394; colistin: $r = 0.69$, $t_{79} = 8.51$, $p < 0.001$; meropenem: $r = 0.17$, $t_{79} = 1.53$, $p =$
168 0.130; tobramycin: $r = 0.58$, $t_{79} = 6.39$, $p < 0.001$). For furanone-antibiotic
169 combinations, there were strong positive correlations between the levels of synergy
170 for the two traits for all drug combinations (ciprofloxacin: $r = 0.34$, $t_{79} = 3.22$, $p =$
171 0.002; colistin: $r = 0.96$, $t_{79} = 32.50$, $p < 0.001$; meropenem: $r = 0.87$, $t_{79} = 15.48$, $p <$
172 0.001; tobramycin: $r = 0.75$, $t_{79} = 10.16$, $p < 0.001$).
173

174 **Antivirulence compounds can restore growth inhibition of antibiotic resistant**
175 **strains**

176 In a next step, we asked whether antivirulence compounds could be used as
177 adjuvants to suppress the growth of antibiotic resistant clones. To address this
178 question, we first experimentally selected and isolated antibiotic resistant clones
179 (AtbR, see methods for details). We then subjected these AtbR clones to antibiotic
180 and combinatorial treatments and compared their growth relative to the ancestral
181 antibiotic-sensitive wildtype. As expected, AtbR clones grew better than the wildtype
182 under antibiotic treatment alone (two-sample t-tests, $-25.9 \leq t_{7\text{-}16} \leq -2.27$, $p < 0.05$ for
183 all treatments). When adding anti-virulence compounds to the antibiotics, we found
184 that growth inhibition of the AtbR clones was restored in seven out of eight drug
185 combinations (Figure 5A). Overall, there were four different inhibition patterns: the
186 addition of antivirulence compounds either (i) did not affect the growth of the
187 antibiotic resistant strain (one case: ciprofloxacin-furanone); (ii) only fully restored
188 growth inhibition at higher anti-virulence compound concentration (five cases: all four
189 combinations with gallium and colistin-furanone); (iii) restored growth inhibition at low

190 but not high anti-virulence compound concentration (one case: meropenem-
191 furanone); or (iv) inhibited growth more than in the antibiotic sensitive wildtype (one
192 case: tobramycin-furanone).
193
194 **Specific drug combinations can reverse selection for antibiotic resistance**
195 We then investigated whether the addition of an antivirulence compound to an
196 antibiotic treatment can influence the spread of AtbR clones in populations of
197 susceptible cells (Figure 5B). Our competition assays revealed that AtbR clones lost
198 against the susceptible wildtype in the absence of antibiotics, confirming that
199 antibiotic resistance is costly (one sample t-tests, $-54.16 \leq t_7 \leq -2.36$, $p \leq 0.050$ for all
200 comparisons). Conversely, AtbR clones always experienced a significant fitness
201 advantage compared to the wildtype under antibiotic treatment (one sample t-test,
202 $3.05 \leq t_7 \leq 12.80$, $p < 0.01$ for all combinations). The addition of antivirulence
203 compounds to the antibiotic treatment had variable and combination-specific effects
204 on the fitness of AtbR clones, which included: (i) three cases where anti-virulence
205 compound addition did not affect the fitness advantage of the AtbR clones
206 (ciprofloxacin-gallium, ciprofloxacin-furanone and colistin-furanone); (ii) two cases
207 where the antivirulence adjuvant further potentiated the spread of AtbR clones
208 (colistin-gallium and meropenem-furanone); and (iii) three cases where the adjuvant
209 reversed selection for antibiotic resistance and thereby hindered the spread of AtbR
210 clones (meropenem-gallium, tobramycin-gallium and tobramycin-furanone). Detailed
211 information on statistical analysis for Figure 5B is reported in Supplementary Table
212 S1.
213
214 **Drug synergy does not predict selection against antibiotic resistance**

215 We examined whether drug interactions, ranging from antagonism to synergy (Figure
216 4) correlate with the relative fitness of the AtbR clones in competition with the
217 antibiotic sensitive wildtype. However, we found no support for such associations
218 (Supplementary Figure S2, ANOVA, growth: $F_{1,48} = 0.65$, $p = 0.422$; virulence factor:
219 $F_{1,48} = 3.10$, $p = 0.082$), but instead observed that variation in fitness patterns was
220 explained by specific drug combinations (antivirulence-antibiotic interaction: $F_{3,48} =$
221 15.76, $p < 0.0001$).
222

223 **Genetic bases of experimentally evolved antibiotic resistance**

224 The whole-genome sequencing of the experimentally evolved AtbR clones revealed
225 a small number of SNPs and INDELs, which are known to be associated with
226 resistance to the respective antibiotics (Table 1). The AtbR clone resistant to
227 ciprofloxacin had mutations in *gyrB*, a gene encoding the DNA gyrase subunit B, the
228 direct target of the antibiotic [36]. In addition, we identified an 18-bp deletion in the
229 *mexR* gene, encoding a multidrug efflux pump repressor [37]. The two AtbR clones
230 resistant to colistin had different mutations in the same target gene *phoQ* (a non-
231 synonymous SNP in one clone versus a 1-bp insertion in addition to a non-
232 synonymous SNP in the other clone). PhoQ is a regulator of the LPS modification
233 operon and mutations in this gene represent the first step in the development of high-
234 level colistin resistance [38]. One AtbR clone resistant to meropenem had a non-
235 synonymous SNP in the coding sequence of *mpl.* This gene encodes a murein
236 tripeptide ligase, which contributes to the overexpression of the beta-lactamase
237 precursor gene *ampC* [39]. The other AtbR clone resistant to meropenem had
238 mutations in three different genes, which can all be linked to antibiotic resistance
239 mechanisms: we found (i) one non-synonymous SNP in *parR*, which encodes a two

240 component response regulator involved in several resistance mechanisms, including
241 drug efflux, porin loss and LPS modification [40]; (ii) 7 mutations in the *PA1874* gene,
242 which encodes an efflux pump [41]; (iii) one non-synonymous SNP in *nalD*, encoding
243 the transcriptional regulator NalD, which regulates the expression of drug-efflux
244 systems [42,43]. Both AtbR clones resistant to tobramycin had non-synonymous
245 SNPs in *fusA1*. This gene encodes the elongation factor G, a key component of the
246 translational machinery. Although aminoglycosides do not directly bind to the
247 elongation factor G and the complete resistance mechanisms is still unknown,
248 mutations in *fusA1* are associated with high resistance to tobramycin and are often
249 found in clinical isolates [44,45].
250

251 ## Discussion

252 In this study, we systematically explored the effects of combining antibiotics with
253 antivirulence compounds as a potentially promising strategy to fight susceptible and
254 antibiotic resistant opportunistic human pathogens. Specifically, we combined four
255 different antibiotics (ciprofloxacin, colistin, meropenem, tobramycin) with two
256 antivirulence compounds (gallium targeting siderophore-mediated iron uptake and
257 furanone C-30 targeting the quorum sensing communication system) in 9x9 drug
258 interaction matrices against the bacterium *P. aeruginosa* as a model pathogen. Our
259 heat maps reveal drug-combination specific interaction patterns. While colistin and
260 tobramycin primarily interacted synergistically with the antivirulence compounds,
261 independent and antagonistic interactions occurred for ciprofloxacin and meropenem
262 in combination with the antivirulence compounds (Figures 3+4). We then used
263 antivirulence compounds as adjuvants and observed that they can restore growth
264 inhibition of antibiotic resistant clones in seven out of eight cases (Figure 5A). Finally,

265 we performed competition assays between antibiotic resistant and susceptible strains
266 under single and combinatorial drug treatments and found that antivirulence
267 compounds can reverse selection for antibiotic resistance in three out of eight cases
268 (Figure 5B). Our results identify antibiotic-antivirulence combinations as a potentially
269 powerful tool to efficiently treat infections of troublesome nosocomial pathogens such
270 as *P. aeruginosa*. Particularly, tobramycin-antivirulence combinations emerged as
271 the top candidate treatments because: (i) drugs interacted synergistically both with
272 regard to growth and virulence factor inhibition; (ii) the antivirulence compounds re-
273 potentiated tobramycin when treating antibiotic resistant clones; and (iii) antivirulence
274 compounds reversed selection for tobramycin resistance.
275
276 Drug synergy is desirable from a clinical perspective because it allows to use lower
277 drug concentrations, thereby minimizing side effects while maintaining treatment
278 efficacy [46,47]. In this context, a number of studies have examined combinations of
279 antibiotics and antivirulence compounds targeting various virulence factors including
280 quorum sensing, iron uptake, and biofilm formation in *P. aeruginosa* [12,13,15–
281 18,22,48–51]. While these studies typically used a handful of concentration
282 combinations and used qualitative measures of synergy, we here present a
283 comprehensive quantitative interaction maps for these two classes of drugs. A key
284 insight of these interaction maps is that specific drug combinations cannot simply be
285 classified as either synergistic or antagonistic. Instead, drug interactions are
286 concentration dependent with most parts of the interaction maps being characterized
287 by independent effects interspersed with hotspots of synergy or antagonism. The
288 strongest effects of synergy and antagonism are often observed at intermediate drug

289 concentrations, which is, in the case of synergy, ideal for developing combinatorial
290 therapies that maximise treatment efficacy while minimizing toxicity for the patient.
291
292 While drug antagonism is considered undesirable from a clinical perspective, work on
293 antibiotic combination therapies has revealed that antagonistic interactions can inhibit
294 the spread of antibiotic resistance [52–54]. The reason behind this phenomenon is
295 that when two drugs antagonize each other, becoming resistant to one drug will
296 remove the antagonistic effect on the second drug, such that the combination
297 treatment will be more effective against the resistant clones [52]. We suspected that
298 such effects might also occur for antagonistic antibiotic-antivirulence treatments.
299 While we indeed observed that combination therapy can reverse selection for
300 resistance in certain cases (Figure 5B), there was no evidence that this effect
301 correlated with the type of drug interaction (Supplementary Figure S2). A possible
302 explanation for the lack of any association is that the antagonism between antibiotics
303 and antivirulence compounds was quite moderate. In contrast, previous work used
304 an extreme case of antagonism, where the effect of one drug was almost completely
305 suppressed in the presence of the second drug [52,54].
306
307 We propose that it is rather the underlying molecular mechanism and not the
308 direction of drug interaction that determines whether selection for antibiotic
309 resistance is reversed or potentiated. For instance, any resistance mechanism that
310 reduces antibiotic entry or increases its efflux could conceivably induce cross-
311 resistance to antivirulence compounds, which should in turn potentiate and not
312 reverse selection for antibiotic resistance. This phenomenon could explain the
313 patterns observed for furanone in combination with ciprofloxacin, colistin and

314 meropenem, where our sequencing analysis revealed mutations in genes regulating
315 efflux pumps, porins and membrane lipopolysaccharide modifications (Table 1).
316 Since furanone needs to enter the cells to become active, these mutations, known to
317 confer resistance to antibiotics [37,38,41], likely also induce resistance to furanone
318 [55].
319
320 Alternatively, competitive interactions between resistant and sensitive pathogens
321 over common resources could compromise the spread of drug resistance, as shown
322 for malaria parasites [56]. In our case, it is plausible to assume that antibiotic
323 resistant clones are healthier than susceptible cells and might therefore produce
324 higher amounts of pyoverdine and proteases under antivirulence treatment. Since
325 these virulence factors are secreted and shared between cells, antibiotic resistant
326 clones take on the role of cooperators: they produce costly virulence factors that are
327 then shared with and exploited by the susceptible cells [26,57,58]. This scenario
328 could apply to tobramycin-gallium/furanone combinations, where resistant clones had
329 mutations in *fusA1* known to be associated with the restoration of protein synthesis
330 [44]. Similar social effects could explain selection reversal in the case of meropenem-
331 gallium combination. Here, the meropenem resistant clone has mutation in *mpl*,
332 which can trigger the overexpression of the β-lactamase *ampC* resistance
333 mechanism [39]. Since β-lactamase enzyme secretion and extracellular antibiotic
334 degradation is itself a cooperative behaviour [59], it could together with the virulence
335 factor sharing described above compromise the spread of the resistant clone.
336 Clearly, all these explanations remain speculative and further studies are required to
337 understand the molecular and evolutionary basis of reversed selection for resistance.
338

339 In summary, drug combination therapies are gaining increased attention as more
340 sustainable strategies to treat infections, limiting the spread of antibiotic resistance
341 [60–63]. They are already applied to a number of diseases, including cancer [64],
342 HIV [65] and tuberculosis infections [66]. Here we probed the efficacy and
343 evolutionary robustness of antibiotics combined with anti-virulence compounds. This
344 is an interesting combination because antibiotic treatments alone face the problem of
345 rapid resistance evolution, whereas antivirulence drugs are evolutionarily more
346 robust but can only disarm and not eliminate pathogens. Combinatorial treatments
347 seem to bring the strengths of the two approaches together: efficient removal of
348 bacteria by the antibiotics combined with disarming and increased evolutionary
349 robustness of the antivirulence compounds. While our findings are promising and
350 could set the stage for a novel class of combinatorial treatments, there are still many
351 steps to take to bring our approach to the clinics. First, it would be important to
352 quantify the rate of resistance evolution directly under the combinatorial treatments to
353 test whether drug combination itself slows down resistance evolution [60]. Second,
354 the various antibiotic-antivirulence combinations must be tested in relevant animal
355 host models, as host conditions including the increased spatial structure inside the
356 body can affect the competitive dynamics between strains, potentially influencing the
357 outcome of the therapy [67,68]. Finally, the observed patterns of drug synergy and
358 reversed selection for resistance are concentration dependent (Figure 4-5), thus
359 requiring detailed research on drug delivery and the pharmacodynamics and
360 pharmacokinetics of combination therapies [54].
361

362 ## Materials and methods

363 ### Bacterial strains

364 For all our experiments, we used *P. aeruginosa* PAO1 (ATCC 15692). In addition to
365 the wildtype PAO1, we further used two isogenic variants tagged with either a
366 constitutively expressed GFP or mCherry fluorescent protein. Both fluorescently
367 tagged strains were directly obtained from the wildtype PAO1 using the miniTn7-
368 system to chromosomally integrate a single stable copy of the marker gene, under
369 the strong constitutive Ptac promoter, at the *att*Tn7 site [69]. The gentamycin
370 resistance cassette, required to select for transformed clones, was subsequently
371 removed using the pFLP2-encoded recombinase [69]. Antibiotic resistant clones
372 used for competition assays were generated through experimental evolution and are
373 listed in Table 1 together with their respective mutations.
374
375 **Media and growth conditions**
376 For all experiments, overnight cultures were grown in 8 ml Lysogeny broth (LB,
377 Sigma Aldrich, Switzerland) in 50 ml Falcon tubes, incubated at 37°C, 220 rpm for 18
378 hours. We washed overnight cultures with 0.8% NaCl solution and adjusted them to
379 OD_{600} = 1 (optical density at 600 nm). Bacteria were further diluted to a final starting
380 OD_{600} = 10^{-3} for all experiments. We used two different media, where the targeted
381 virulence factors (pyoverdine or protease) are important. For pyoverdine, we used
382 iron-limited CAA (CAA+Tf) [0.5% casamino acids, 5 mM $K_2HPO_4 \cdot 3H_2O$, 1 mM
383 $MgSO_4 \cdot 7H_2O$], buffered at neutral pH with 25 mM HEPES buffer and supplemented
384 with 100 µg/ml human apo-transferrin to chelate iron and 20 mM $NaHCO_3$ as a co-
385 factor. As an iron-rich control medium, we used CAA supplemented with 25 mM
386 HEPES and 20 µM $FeCl_3$, but without apo-transferrin and 20 mM $NaHCO_3$ to create
387 conditions that do not require pyoverdine for growth [70].
388

389 For QS-regulated proteases, we used casein medium (CAS) [0.5% casein, 5 mM
390 $K_2HPO_4 \cdot 3H_2O$, 1 mM $MgSO_4 \cdot 7H_2O$], supplemented with 25 mM HEPES buffer and
391 0.05% CAA. In this medium, proteases are required to digest the casein. A small
392 amount of CAA was added to allow cultures to have a growth kick start prior to
393 protease secretion [71]. As a control, we used CAA supplemented with 25 mM
394 HEPES buffer, a medium in which proteases are not required. All chemicals were
395 purchased from Sigma Aldrich, Switzerland. The CAS medium is intrinsically turbid
396 due to the poor solubility of casein, which can interfere with the growth kinetics
397 measured via optical density (Supplementary Figure S3A). To solve this issue, we
398 used mCherry fluorescence intensity as a reliable proxy for growth in CAS
399 (Supplementary Figure S3B-C).
400

401 **Single drug growth and virulence factor inhibition curves**

402 To determine the activity range of each antibiotic (ciprofloxacin, colistin, meropenem,
403 tobramycin) and antivirulence drug (gallium as $GaNO_3$ and furanone C-30), we
404 subjected PAO1 bacterial cultures to two different 7-step serial dilutions for each
405 antibacterial. Ciprofloxacin: 0-4 µg/ml; colistin: 0-0.4 µg/ml in CAA+Tf and 0-20 µg/ml
406 in CAS; meropenem: 0-14 µg/ml; tobramycin: 0-8 µg/ml; gallium: 0-200 µM; furanone
407 C-30: 0-390 µM. All antibacterials were purchased from Sigma Aldrich, Switzerland.
408 Overnight cultures were prepared and diluted as explained above and then added
409 into 200 µl of media on 96-well plates with six replicates for each drug concentration.
410 Plates were incubated statically at 37°C and growth was measured either as OD_{600}
411 (in CAA+Tf) or mCherry fluorescence (excitation 582 nm, emission 620 nm in CAS)
412 after 48 hours using a Tecan Infinite M-200 plate reader (Tecan Group Ltd.,
413 Switzerland). Control experiments (Supplementary Figure S4) confirmed that

414 endpoint OD_{600} or mCherry measurements showed strong linear correlations (0.858
415 < R^2 < 0.987) with the growth integral (area under the growth curve), which is a good
416 descriptor of the overall inhibitory effects covering the entire growth period [72].
417
418 At this time point, we further quantified pyoverdine production through its natural
419 fluorescence (excitation 400 nm, emission 460 nm) and protease production in the
420 cell-free supernatant using the protease azocasein assay (adapted from [73]
421 shortening incubation time to 30 min). The two metals, gallium and bromine (in
422 Furanone C-30), alter the fluorescence levels of pyoverdine and mCherry in a
423 concentration dependent manner. To account for this effect, we established
424 calibration curves and corrected all fluorescence measures accordingly (as described
425 in Supplementary Figure S5).
426
427 **Antibiotic-antivirulence combination assays**
428 From the single drug dose-response curves, we chose for each drug nine
429 concentrations (including no drugs) to cover the entire activity range in each medium
430 including no, intermediate and strong inhibitory growth effects on PAO1.
431 (Supplementary Table S2). We then combined these drug concentrations in a 9x9
432 matrix for each of the eight antibiotic-antivirulence pairs, and repeated the growth
433 experiment for all combinations in six-fold replication, exactly as described above.
434 After 48 hours of incubation, we measured growth and virulence factor production
435 following the protocols described above.
436
437 **Synergy degree of drug-combinations**

438 We used the Bliss independence model to calculate the degree of synergy (S), for
439 both growth and virulence factor inhibition, for each of the antibiotic-antivirulence
440 combinations [74–76]. We used the formula $S = f_{X,0} \cdot f_{0,Y} - f_{X,Y}$, where $f_{X,0}$ is the
441 growth (or virulence factor production) level measured under antibiotic exposure at
442 concentration X; $f_{0,Y}$ is the growth (or virulence factor production) level measured
443 under antivirulence exposure at concentration Y; and $f_{X,Y}$ is the growth (or virulence
444 factor production) level measured under the combinatorial treatment at
445 concentrations X and Y. If $S = 0$ then the two drugs act independently. Conversely,
446 $S < 0$ indicates antagonistic drug interactions, while $S > 0$ indicates synergy.
447

448 **Experimental evolution under antibiotic treatment**

449 To select for antibiotic resistant clones, we exposed overnight cultures of PAO1
450 wildtype (initial $OD_{600} = 10^{-4}$) to each of the four antibiotics in LB medium (antibiotic
451 concentrations, ciprofloxacin: 0.15 µg/ml; colistin: 0.5 µg/ml; meropenem: 0.8 µg/ml;
452 tobramycin: 1 µg/ml) in six-fold replication. These antibiotic concentrations initially
453 caused a 70-90% reduction in PAO1 growth compared to untreated cultures,
454 conditions that imposed strong selection for the evolution of resistance. The evolution
455 experiment ran for seven days, whereby we diluted bacterial cultures and transferred
456 them to fresh medium with the respective treatment with a dilution factor of 10^{-4},
457 every 24 hours. At the end of each growth cycle, we measured growth (OD_{600}) of the
458 evolving lineages using a SpectraMax® Plus 384 plate reader (Molecular Devices,
459 Switzerland).
460

461 **Phenotypic and genetic characterization of resistance**

462 Following experimental evolution, we screened the evolved lines for the presence of
463 antibiotic resistant clones. For each antibiotic we plated four evolved lines on LB
464 plates and isolated single clones, which we then exposed in liquid culture to the
465 antibiotic concentration they experienced during experimental evolution. Among
466 those that showed growth restoration (compared to the untreated wildtype), we
467 picked two random clones originating from different lineages per antibiotic for further
468 analysis. We had to adjust our sampling design in two cases. First, only one
469 population survived our ciprofloxacin treatment and thus only one resistant clone
470 could be picked for this antibiotic. Second, clones evolved under colistin treatment
471 grew very poorly in CAS medium and therefore we included an experimentally
472 evolved colistin resistant clone from a previous study, which did not show
473 compromised growth in CAS (see [73] for a description on the experimental
474 evolution). Altogether, we had seven clones for which we re-established the drug-
475 response curves (Supplementary Figure S6) in either CAA+Tf or CAS (one clone per
476 antibiotic was allocated to one of the two media, except for ciprofloxacin).
477
478 We further isolated the genomic DNA of the selected evolved antibiotic resistant
479 clones and sequenced their genomes. We used the GenElute Bacterial Genomic
480 DNA kit (Sigma Aldrich) for DNA isolation. DNA concentrations were assayed using
481 the Quantifluor dsDNA sample kit (Promega, Switzerland). Samples were sent to the
482 Functional Genomics Center Zurich for library preparation (TruSeq DNA Nano) and
483 sequencing on the Illumina MiSeq platform with v2 reagents and pair-end 150 bp
484 reads. In a first step, we mapped the sequences of our ancestral wildtype PAO1
485 strain (ENA accession number: ERS1983671) to the *Pseudomonas aeruginosa*
486 PAO1 reference genome (NCBI accession number: NC_002516) with snippy

487 (https://github.com/tseemann/snippy) to obtain a list with variants that were already
488 present at the beginning of the experiment. Next, we quality filtered the reads of the
489 evolved clones with trimmomatic [77], mapped them to the reference genome and
490 called variants using snippy. Detected variants were quality filtered and variants
491 present in the ancestor strain were excluded from the dataset using vcftools [78]. The
492 mapping files generated in this study are deposited in the European Nucleotide
493 Archive (ENA) under the study accession number PRJEB32766.
494

495 **Competition experiments between sensitive and resistant clones**

496 To examine the conditions under which antibiotic resistant clones can spread, we
497 competed the sensitive wildtype PAO1 (tagged with GFP) against the experimentally
498 evolved antibiotic resistant clones (Table 1) under five different conditions: (i) no drug
499 treatment; (ii) antibiotic alone; (iii)-(v) antibiotic combined with three different
500 concentrations of the antivirulence compound. Antibiotic concentrations are listed in
501 the Supplementary Table S3, while antivirulence concentrations were as follows,
502 gallium: 1.56 μM (low), 6.25 μM (medium), 12.5 μM (high); furanone: 6.3 μM (low),
503 22.8 μM (medium), 51.4 μM (high). Bacterial overnight cultures were prepared and
504 diluted as described above. Competitions were initiated with a mixture of 90%
505 sensitive wildtype cells and 10% resistant clones to mimic a situation where
506 resistance is still relatively rare. Mixes alongside with monocultures of all strains were
507 inoculated in either 200 μl of CAA+Tf or CAS under all the five treatment regimes.
508 We used flow cytometry to assess strain frequency prior and after a 24 hours
509 competition period at 37°C static (Supplementary Figure S7). Specifically, bacterial
510 cultures were diluted in 1X phosphate buffer saline (PBS, Gibco, ThermoFisher,
511 Switzerland) and frequencies were measured with a LSRII Fortessa cell analyzer (BD

512 Bioscience, Switzerland. GFP channel, laser: 488 nm, mirror: 505LP, filter: 530/30;
513 side and forward scatter: 200 V threshold; events recorded with CS&T settings) at
514 the Cytometry Facility of the University of Zurich. We recorded 50'000 events before
515 competitions and used a high-throughput sampler device (BD Bioscience) to record
516 all events in a 5 µl-volume after competition. Since antibacterials can kill and thereby
517 quench the GFP signal in tagged cells, we quantified dead cells using the propidium
518 iodide (PI) stain (2 µl of 0.5 mg/ml solution) with flow cytometry (for PI fluorescence:
519 laser: 561 nm, mirror: 600LP, filter: 610/20).
520
521 We used the software FlowJo (BD Bioscience) to analyse data from flow cytometry
522 experiments. We followed a three-step gating strategy: (i) we separated bacterial
523 cells from media and noise background by using forward and side scatter values as a
524 proxy for particle size; (ii) within this gate, we then distinguished live from dead cells
525 based on the PI staining; (iii) finally, we separated live cells into either GFP positive
526 and negative populations. Fluorescence thresholds were set using appropriate
527 control samples: isopropanol-killed cells for PI positive staining and untagged-PAO1
528 cells for GFP-negative fluorescence. We then calculated the relative fitness of the
529 antibiotic resistant clone as $\ln(v) = \ln\{[a_{24}\times(1-a_0)]/[a_0\times(1-a_{24})]\}$, where a_0 and a_{24} are
530 the frequencies of the resistant clone at the beginning and at the end of the
531 competition, respectively [79]. Values of $\ln(v) < 0$ or $\ln(v) > 0$ indicate whether the
532 frequency of antibiotic resistant clones decreased or increased relative to the
533 sensitive PAO1-GFP strain. To check for fitness effects caused by the fluorescent
534 tag, we included a control competition, where we mixed PAO1-GFP with the
535 untagged PAO1 in a 9:1 ratio for all treatment conditions. We noted that high drug
536 concentrations significantly curbed bacterial growth, which reduced the number of

537 events that could be measured with flow cytometry. This growth reduction increased
538 noise relative to the signal, leading to an overestimation of the GFP-negative
539 population in the mix. To correct for this artefact, we established calibration curves
540 (described by asymptotic functions, Supplementary Table S2) for how the relative
541 fitness of PAO1-untagged varies as a function of cell density in control competitions
542 with PAO1-GFP.
543
544 **Statistical analysis**
545 All statistical analyses were performed with RStudio v. 3.3.0 [80]. We fitted individual
546 dose response curves with either log-logistic or Weibull functions using the drc
547 package [81], while dose response curves under combination treatment were fitted
548 using spline functions. We used Pearson correlation coefficients to test for significant
549 associations between the degree of synergy in growth and virulence factor inhibition.
550 We used Welch's two-sample t-test to compare growth between the sensitive
551 wildtype PAO1 and the resistant clones under antibiotic treatment. To compare the
552 relative fitness of resistant clones to the reference zero line, we used one sample t-
553 tests. Finally, we used analysis of variance (ANOVA) to compare: (a) the growth of
554 sensitive and resistant clones across combination treatments; (b) the relative fitness
555 of evolved clones across treatments, and (c) whether the outcome of the competition
556 experiment is associated with the degree of synergy of the drug combinations. Where
557 necessary, p-values were adjusted for multiple comparisons using the false discovery
558 rate method.

Acknowledgments

We thank Roland Regös and Désirée Bäder for advice on the Bliss model; Alex Hall, Roland Regös and Frank Schreiber for comments on the manuscripts; Ingrid Mignot and David Wilson for experimental support; Selina Niggli, Priyanikha Jayakumar and the Flow Cytometry Facility (University of Zurich) for support with flow cytometry experiments; and the Functional Genomics Center Zurich for technical support with the strain sequencing.

Funding

This project has received funding from the Swiss National Science Foundation (grant no. 31003A_182499 to RK) and the European Research Council (ERC) under the European Union's Horizon 2020 research and innovation programme (grant agreement no. 681295 to RK).

Competing Interests

The authors have no competing interests to declare.

575 ## References

576 1. Rossolini GM, Arena F, Pecile P, Pollini S. Update on the antibiotic resistance
577 crisis. Curr Opin Pharmacol. Elsevier Ltd; 2014;18: 56–60.
578 doi:10.1016/j.coph.2014.09.006
579 2. World Health Organization (WHO). Antimicrobial resistance: Global Health
580 Report on Surveillance [Internet]. Bulletin of the World Health Organization.
581 2014. doi:10.1007/s13312-014-0374-3
582 3. O'Neill J. Antimicrobial Resistance: Tackling a crisis for the health and wealth
583 of nations. Review on Antimicrobial Resistance. London; 2014.
584 doi:10.1038/510015a
585 4. Tacconelli E, Carrara E, Savoldi A, Harbarth S, Mendelson M, Monnet DL, et
586 al. Discovery, research, and development of new antibiotics: the WHO priority
587 list of antibiotic-resistant bacteria and tuberculosis. Lancet Infect Dis. Elsevier;
588 2018;18: 318–327. doi:10.1016/S1473-3099(17)30753-3
589 5. Laxminarayan R, Matsoso P, Pant S, Brower C, Rottingen J-A, Klugman K, et
590 al. Access to effective antimicrobials: a worldwide challenge. Lancet. England;
591 2016;387: 168–175. doi:10.1016/S0140-6736(15)00474-2
592 6. Dickey SW, Cheung GYC, Otto M. Different drugs for bad bugs: antivirulence
593 strategies in the age of antibiotic resistance. Nat Rev Drug Discov. 2017;16: 1–
594 15. doi:10.1038/nrd.2017.23
595 7. Brown D. Antibiotic resistance breakers: can repurposed drugs fill the antibiotic
596 discovery void? Nat Rev Drug Discov. 2015;14: 821–832. doi:10.1038/nrd4675
597 8. Allen RC, Popat R, Diggle SP, Brown SP. Targeting virulence: can we make
598 evolution-proof drugs? Nat Rev Microbiol. 2014;12: 300–308.
599 doi:10.1038/nrmicro3232

600 9. Vale PF, Fenton A, Brown SP. Limiting Damage during Infection: Lessons from
601 Infection Tolerance for Novel Therapeutics. PLOS Biol. 2014;12.
602 doi:10.1371/journal.pbio.1001769
603 10. Vale PF, McNally L, Doeschl-Wilson A, King KC, Popat R, Domingo-Sananes
604 MR, et al. Beyond killing. Evol Med Public Heal. 2016;2016: 148–157.
605 doi:10.1093/emph/eow012
606 11. Ternent L, Dyson RJ, Krachler AM, Jabbari S. Bacterial fitness shapes the
607 population dynamics of antibiotic-resistant and -susceptible bacteria in a model
608 of combined antibiotic and anti-virulence treatment. J Theor Biol. Elsevier;
609 2015;372: 1–11. doi:10.1016/j.jtbi.2015.02.011
610 12. Hentzer M, Wu H, Andersen JB, Riedel K, Rasmussen TB, Bagge N, et al.
611 Attenuation of Pseudomonas aeruginosa virulence by quorum sensing
612 inhibitors. EMBO J. 2003;22: 3803–3815. doi:10.1093/emboj/cdg366
613 13. Banin E, Lozinski A, Brady KM, Berenshtein E, Butterfield PW, Moshe M, et al.
614 The potential of desferrioxamine-gallium as an anti-*Pseudomonas* therapeutic
615 agent. Proc Natl Acad Sci U S A. 2008;105: 16761–16766.
616 doi:10.1073/pnas.0808608105
617 14. Zeng Z, Qian L, Cao L, Tan H, Huang Y, Xue X, et al. Virtual screening for
618 novel quorum sensing inhibitors to eradicate biofilm formation of Pseudomonas
619 aeruginosa. Appl Microbiol Biotechnol. 2008;79: 119–126. doi:10.1007/s00253-
620 008-1406-5
621 15. Jakobsen TH, Van Gennip M, Phipps RK, Shanmugham MS, Christensen LD,
622 Alhede M, et al. Ajoene, a sulfur-rich molecule from garlic, inhibits genes
623 controlled by quorum sensing. Antimicrob Agents Chemother. 2012;56: 2314–
624 2325. doi:10.1128/AAC.05919-11

625 16. Michaud G, Visini R, Bergmann M, Salerno G, Bosco R, Gillon E, et al.
626 Overcoming antibiotic resistance in Pseudomonas aeruginosa biofilms using
627 glycopeptide dendrimers. Chem Sci. 2016;7: 166–182. doi:10.1039/c5sc03635f
628 17. Goss CH, Kaneko Y, Khuu L, Anderson GD, Ravishankar S, Aitken ML, et al.
629 Gallium disrupts bacterial iron metabolism and has therapeutic effects in mice
630 and humans with lung infections. Sci Transl Med. 2018;10: eaat7520.
631 18. Kirienko DR, Kang D, Kirienko N V. Novel Pyoverdine Inhibitors Mitigate
632 Pseudomonas aeruginosa Pathogenesis. Front Microbiol. 2019;9: 3317.
633 19. Breidenstein EBM, de la Fuente-Núñez C, Hancock REW. *Pseudomonas*
634 *aeruginosa*: all roads lead to resistance. Trends Microbiol. 2011;19: 419–426.
635 doi:10.1016/j.tim.2011.04.005
636 20. Gellatly SL, Hancock REW. Pseudomonas aeruginosa: New insights into
637 pathogenesis and host defenses. Pathog Dis. 2013;67: 159–173.
638 doi:10.1111/2049-632X.12033
639 21. Hentzer M, Riedel K, Rasmussen TB, Heydorn A, Andersen JB, Parsek MR, et
640 al. Inhibition of quorum sensing in Pseudomonas aeruginosa biofilm bacteria
641 by a halogenated furanone compound Inhibition of quorum sensing in
642 Pseudomonas aeruginosa biofilm bacteria by a halogenated furanone
643 compound. Microbiology. 2002;148: 87–102. doi:10.1099/00221287-148-1-87
644 22. Rasmussen TB, Bjarnsholt T, Skindersoe ME, Hentzer M, Kristoffersen P, Köte
645 M, et al. Screening for Quorum-Sensing Inhibitors (QSI) by Use of a Novel
646 Genetic System, the QSI Selector. J Bacteriol. 2005;187: 1799 LP-1814.
647 doi:10.1128/JB.187.5.1799-1814.2005
648 23. Defoirdt T. Quorum-Sensing Systems as Targets for Antivirulence Therapy.
649 Trends Microbiol. Elsevier Ltd; 2018;26: 313–328.

650 doi:10.1016/j.tim.2017.10.005

651 24. Kaneko Y, Thoendel M, Olakanmi O, Britigan BE, Singh PK. The transition
652 metal gallium disrupts *Pseudomonas aeruginosa* iron metabolism and has
653 antimicrobial and antibiofilm activity. J Clin Invest. 2007;117: 877–888.
654 doi:10.1172/JCI30783

655 25. Smith DJ, Lamont IL, Anderson GJ, Reid DW. Targeting iron uptake to control
656 *Pseudomonas aeruginosa* infections in cystic fibrosis. Eur Respir J. 2013;42:
657 1723–36. doi:10.1183/09031936.00124012

658 26. Ross-Gillespie A, Weigert M, Brown SP, Kümmerli R. Gallium-mediated
659 siderophore quenching as an evolutionarily robust antibacterial treatment. Evol
660 Med Public Heal. 2014;2014: 18–29. doi:10.1093/emph/eou003

661 27. Imperi F, Massai F, Facchini M, Frangipani E, Visaggio D, Leoni L, et al.
662 Repurposing the antimycotic drug flucytosine for suppression of *Pseudomonas*
663 *aeruginosa* pathogenicity. Proc Natl Acad Sci U S A. 2013;110: 7458–63.
664 doi:10.1073/pnas.1222706110

665 28. DeLeon K, Balldin F, Watters C, Hamood A, Griswold J, Sreedharan S, et al.
666 Gallium Maltolate Treatment Eradicates *Pseudomonas aeruginosa* Infection in
667 Thermally Injured Mice. Antimicrob Agents Chemother. 2009;53: 1331–1337.
668 doi:10.1128/AAC.01330-08

669 29. Kelson AB, Carnevali M, Truong-Le V. Gallium-based anti-infectives: targeting
670 microbial iron-uptake mechanisms. Curr Opin Pharmacol. 2013;13: 707–716.
671 doi:10.1016/j.coph.2013.07.001

672 30. Bonchi C, Imperi F, Minandri F, Visca P, Frangipani E. Repurposing of gallium-
673 based drugs for antibacterial therapy. BioFactors. 2014;40: 303–312.
674 doi:10.1002/biof.1159

675 31. Hijazi S, Visca P, Frangipani E. Gallium-Protoporphyrin IX Inhibits
676 *Pseudomonas aeruginosa* Growth by Targeting Cytochromes. Front Cell Infect
677 Microbiol. 2017;7: 1–15. doi:10.3389/fcimb.2017.00012
678 32. Hijazi S, Visaggio D, Pirolo M, Frangipani E, Bernstein L, Visca P. Antimicrobial
679 activity of gallium compounds on ESKAPE pathogens. Front Cell Infect
680 Microbiol. 2018;8: 316.
681 33. Manny AJ, Kjelleberg S, Kumar N, de Nys R, Read RW, Steinberg P.
682 Reinvestigation of the sulfuric acid-catalysed cyclisation of brominated 2-
683 alkyllevulinic acids to 3-alkyl-5-methylene-2 (5H)-furanones. Tetrahedron.
684 Elsevier; 1997;53: 15813–15826.
685 34. Manefield M, de Nys R, Kumar N, Read R, Givskov M, Steinberg P, et al.
686 Evidence that halogenated furanones from Delisea pulchra inhibit acylated
687 homoserine lactone (AHL)-mediated gene expression by displacing the AHL
688 signal from its receptor protein. Microbiology. 1999;145 (Pt 2: 283–291.
689 35. Bassetti M, Vena A, Croxatto A, Righi E, Guery B. How to manage
690 Pseudomonas aeruginosa infections. Drugs Context. England; 2018;7: 212527.
691 doi:10.7573/dic.212527
692 36. Rehman A, Patrick WM, Lamont IL. Mechanisms of ciprofloxacin resistance in
693 pseudomonas aeruginosa: New approaches to an old problem. J Med
694 Microbiol. 2019;68: 1–10. doi:10.1099/jmm.0.000873
695 37. Poole K, Neshat S, Heinrichs DE, Zhao Q, Tetro K, Bianco N. Expression of
696 the multidrug resistance operon mexA-mexB-oprM in Pseudomonas
697 aeruginosa: mexR encodes a regulator of operon expression. Antimicrob
698 Agents Chemother. 2018;40: 2021–2028. doi:10.1128/aac.40.9.2021
699 38. Jochumsen N, Paulander W, Jensen RL, Folkesson A, Molin S, Jelsbak L, et

700 al. The evolution of antimicrobial peptide resistance in Pseudomonas
701 aeruginosa is shaped by strong epistatic interactions. Nat Commun. 2016;7:
702 13002. doi:10.1038/ncomms13002
703 39. Tsutsumi Y, Tomita H, Tanimoto K. Identification of Novel Genes Responsible
704 for Overexpression of ampC in Pseudomonas aeruginosa PAO1 . Antimicrob
705 Agents Chemother. 2013;57: 5987–5993. doi:10.1128/aac.01291-13
706 40. Muller C, Plésiat P, Jeannot K. A Two-Component Regulatory System
707 Interconnects Resistance to Polymyxins, Aminoglycosides, Fluoroquinolones,
708 and beta-Lactams in Pseudomonas aeruginosa. Antimicrob Agents
709 Chemother. 2011;55: 1211–1221. doi:10.1128/AAC.01252-10
710 41. Zhang L, Mah TF. Involvement of a novel efflux system in biofilm-specific
711 resistance to antibiotics. J Bacteriol. 2008;190: 4447–4452.
712 doi:10.1128/JB.01655-07
713 42. Quale J, Bratu S, Gupta J, Landman D. Interplay of efflux system, ampC, and
714 oprD expression in carbapenem resistance of Pseudomonas aeruginosa
715 clinical isolates. Antimicrob Agents Chemother. 2006;50: 1633–1641.
716 doi:10.1128/AAC.50.5.1633-1641.2006
717 43. Pan Y ping, Xu Y hong, Wang Z xin, Fang Y ping, Shen J lu. Overexpression of
718 MexAB-OprM efflux pump in carbapenem-resistant Pseudomonas aeruginosa.
719 Arch Microbiol. Springer Berlin Heidelberg; 2016;198: 565–571.
720 doi:10.1007/s00203-016-1215-7
721 44. Bolard A, Plesiat P, Jeannot K. Mutations in gene fusA1 as a novel mechanism
722 of aminoglycoside resistance. 2017; 33–3. doi:10.1128/AAC.01835-17
723 45. López-Causapé C, Rubio R, Cabot G, Oliver A. Evolution of the *Pseudomonas*
724 *aeruginosa* Aminoglycoside Mutational Resistome In Vitro and in the Cystic

725 Fibrosis Setting. Antimicrob Agents Chemother. 2018;62: e02583-17.
726 doi:10.1128/AAC.02583-17
727 46. Acar JF. Antibiotic synergy and antagonism. Med Clin North Am. 2000;84:
728 1391–1406. doi:https://doi.org/10.1016/S0025-7125(05)70294-7
729 47. Lehár J, Krueger AS, Avery W, Heilbut AM, Johansen LM, Price ER, et al.
730 Synergistic drug combinations tend to improve therapeutically relevant
731 selectivity. Nat Biotechnol. 2009;27: 659–666. doi:10.1038/nbt.1549
732 48. Alkawash MA, Soothill JS, Schiller NL. Alginate lyase enhances antibiotic
733 killing of mucoid Pseudomonas aeruginosa in biofilms. Apmis. 2006;114: 131–
734 138. doi:10.1111/j.1600-0463.2006.apm_356.x
735 49. Moreau-Marquis S, O'Toole GA, Stanton BA. Tobramycin and FDA-approved
736 iron chelators eliminate Pseudomonas aeruginosa biofilms on cystic fibrosis
737 cells. Am J Respir Cell Mol Biol. 2009;41: 305–313. doi:10.1165/rcmb.2008-
738 0299OC
739 50. Moreau-Marquis S, Coutermarsh B, Stanton BA. Combination of
740 hypothiocyanite and lactoferrin (ALX-109) enhances the ability of tobramycin
741 and aztreonam to eliminate Pseudomonas aeruginosa biofilms growing on
742 cystic fibrosis airway epithelial cells. J Antimicrob Chemother. 2015;70: 160–
743 166. doi:10.1093/jac/dku357
744 51. Luo J, Dong B, Wang K, Cai S, Liu T, Cheng X, et al. Baicalin inhibits biofilm
745 formation, attenuates the quorum sensing-controlled virulence and enhances
746 Pseudomonas aeruginosa clearance in a mouse peritoneal implant infection
747 model. PLOS One. 2017;12: 1–32.
748 52. Chait R, Craney A, Kishony R. Antibiotic interactions that select against
749 resistance. Nature. 2007;446: 668–671. doi:10.1038/nature05685

750 53. Hegreness M, Shoresh N, Damian D, Hartl D, Kishony R. Accelerated
751 evolution of resistance in multidrug environments. Proc Natl Acad Sci. National
752 Academy of Sciences; 2008;105: 13977–13981.
753 doi:10.1073/PNAS.0805965105
754 54. Baym M, Stone LK, Kishony R. Multidrug evolutionary strategies to reverse
755 antibiotic resistance. Science. 2016;351. doi:10.1126/science.aad3292
756 55. Maeda T, García-Contreras R, Pu M, Sheng L, Garcia LR, Tomás M, et al.
757 Quorum quenching quandary: resistance to antivirulence compounds. ISME J.
758 2012;6: 493–501. doi:10.1038/ismej.2011.122
759 56. Wale N, Sim DG, Jones MJ, Salathe R, Day T, Read AF. Resource limitation
760 prevents the emergence of drug resistance by intensifying within-host
761 competition. Proc Natl Acad Sci. 2017; 201715874.
762 doi:10.1073/pnas.1715874115
763 57. Mellbye B, Schuster M. The sociomicrobiology of antivirulence drug resistance:
764 a proof of concept. MBio. 2011;2: e00131-11. doi:10.1128/mBio.00131-11
765 58. Gerdt JP, Blackwell HE. Competition Studies Confirm Two Major Barriers That
766 Can Preclude the Spread of Resistance to Quorum-Sensing Inhibitors in
767 Bacteria. ACS Chem Biol. 2014;9: 2291–2299. doi:10.1021/cb5004288
768 59. Vega NM, Gore J. Collective antibiotic resistance: Mechanisms and
769 implications. Curr Opin Microbiol. Elsevier Ltd; 2014;21: 28–34.
770 doi:10.1016/j.mib.2014.09.003
771 60. Fischbach MA. Combination therapies for combating antimicrobial resistance.
772 Curr Opin Microbiol. Elsevier Ltd; 2011;14: 519–523.
773 doi:10.1016/j.mib.2011.08.003
774 61. Silver LL. Challenges of Antibacterial Discovery. Clin Microbiol Rev. 2011;24:

775 71–109. doi:10.1128/CMR.00030-10
776 62. Tepekule B, Uecker H, Derungs I, Frenoy A, Bonhoeffer S. Modeling antibiotic
777 treatment in hospitals: A systematic approach shows benefits of combination
778 therapy over cycling, mixing, and mono-drug therapies. PLOS Comput Biol.
779 2017;13: 1–22. doi:10.1371/journal.pcbi.1005745
780 63. Tyers M, Wright GD. Drug combinations: a strategy to extend the life of
781 antibiotics in the 21st century. Nat Rev Microbiol. Springer US; 2019;17: 141–
782 155. doi:10.1038/s41579-018-0141-x
783 64. Bayat Mokhtari R, Homayouni TS, Baluch N, Morgatskaya E, Kumar S, Das B,
784 et al. Combination therapy in combating cancer. Oncotarget. United States;
785 2017;8: 38022–38043. doi:10.18632/oncotarget.16723
786 65. Cihlar T, Fordyce M. Current status and prospects of HIV treatment. Curr Opin
787 Virol. 2016;18: 50–56. doi:https://doi.org/10.1016/j.coviro.2016.03.004
788 66. Ginsberg AM, Spigelman M. Challenges in tuberculosis drug research and
789 development. Nat Med. United States; 2007;13: 290–294.
790 doi:10.1038/nm0307-290
791 67. Zhou L, Slamti L, Nielsen-LeRoux C, Lereclus D, Raymond B. The Social
792 Biology of Quorum Sensing in a Naturalistic Host Pathogen System. Curr Biol.
793 Cell Press; 2014;24: 2417–2422. doi:10.1016/J.CUB.2014.08.049
794 68. Rezzoagli C, Granato E, Kuemmerli R. In vivo microscopy reveals the impact
795 of Pseudomonas aeruginosa social interactions on host colonization. ISME J.
796 2019;
797 69. Choi K-H, Schweizer HP. mini-Tn7 insertion in bacteria with single attTn7 sites:
798 example *Pseudomonas aeruginosa*. Nat Protoc. 2006;1: 153–161.
799 doi:10.1038/nprot.2006.24

800 70. Kümmerli R, Jiricny N, Clarke LS, West SA, Griffin AS. Phenotypic plasticity of
801 a cooperative behaviour in bacteria. J Evol Biol. 2009;22: 589–598.
802 doi:10.1111/j.1420-9101.2008.01666.x
803 71. Özkaya Ö, Balbontín R, Gordo I, Xavier KB. Cheating on Cheaters Stabilizes
804 Cooperation in *Pseudomonas aeruginosa*. Curr Biol. 2018;26: 2070–2080.
805 doi:10.1016/j.cub.2018.04.093
806 72. Ocampo PS, Lázár V, Papp B, Arnoldini M, Zur Wiesch PA, Busa-Fekete R, et
807 al. Antagonism between bacteriostatic and bactericidal antibiotics is prevalent.
808 Antimicrob Agents Chemother. 2014;58: 4573–4582. doi:10.1128/AAC.02463-
809 14
810 73. Rezzoagli C, Wilson D, Weigert M, Wyder S, Kümmerli R. Probing the
811 evolutionary robustness of two repurposed drugs targeting iron uptake in
812 *Pseudomonas aeruginosa*. Evol Med Public Heal. 2018;1: 246–259.
813 doi:10.1093/emph/eoy026
814 74. Morones-Ramirez JR, Winkler JA, Spina CS, Collins JJ. Silver Enhances
815 Antibiotic Activity Against Gram-Negative Bacteria. Sci Transl Med. 2013;5: 1–
816 12.
817 75. Baeder DY, Yu G, Hozé N, Rolff J, Regoes RR. Antimicrobial combinations:
818 Bliss independence and Loewe additivity derived from mechanistic multi-hit
819 models. Philos Trans R Soc B Biol Sci. 2016;371. Available:
820 http://rstb.royalsocietypublishing.org/content/371/1695/20150294.abstract
821 76. Barbosa C, Beardmore R, Schulenburg H, Jansen G. Antibiotic combination
822 efficacy (ACE) networks for a Pseudomonas aeruginosa model. PLOS Biol.
823 2018;16: 1–25.
824 77. Bolger AM, Lohse M, Usadel B. Trimmomatic: a flexible trimmer for Illumina

825 sequence data. Bioinformatics. 2014;30: 2114–2120.
826 doi:10.1093/bioinformatics/btu170
827 78. Danecek P, Auton A, Abecasis G, Albers CA, Banks E, DePristo MA, et al. The
828 variant call format and VCFtools. Bioinformatics. 2011/06/07. Oxford University
829 Press; 2011;27: 2156–2158. doi:10.1093/bioinformatics/btr330
830 79. Ross-Gillespie A, Gardner A, West SA, Griffin AS. Frequency dependence and
831 cooperation: theory and a test with bacteria. Am Nat. 2007;170: 331–342.
832 doi:10.1086/519860
833 80. R Development Core Team. R: A language and environment for statistical
834 computing. R Foundation for Statistical Computing. Vienna, Austria; 2013.
835 81. Ritz C, Baty F, Streibig JC, Gerhard D. Dose-Response Analysis Using R.
836 PLOS One. 2015;10: 1–13. doi:10.1371/journal.pone.0146021
837 82. Higgins PG, Fluit AC, Milatovic D, Verhoef J, Schmitz FJ. Mutations in GyrA,
838 ParC, MexR and NfxB in clinical isolates of Pseudomonas aeruginosa. Int J
839 Antimicrob Agents. 2003;21: 409–413. doi:10.1016/S0924-8579(03)00009-8
840 83. Miller AK, Brannon MK, Stevens L, Johansen HK, Selgrade SE, Miller SI, et al.
841 PhoQ mutations promote lipid A modification and polymyxin resistance of
842 Pseudomonas aeruginosa found in colistin-treated cystic fibrosis patients.
843 Antimicrob Agents Chemother. 2011;55: 5761–5769. doi:10.1128/AAC.05391-
844 11
845 84. Lee JY, Park YK, Chung ES, Na IY, Ko KS. Evolved resistance to colistin and
846 its loss due to genetic reversion in Pseudomonas aeruginosa. Sci Rep. Nature
847 Publishing Group; 2016;6: 1–13. doi:10.1038/srep25543
848 85. Barrow K, Kwon DH. Alterations in two-component regulatory systems of
849 phoPQ and pmrAB are associated with polymyxin B resistance in clinical

850 isolates of Pseudomonas aeruginosa. Antimicrob Agents Chemother. 2009;53:
851 5150–5154. doi:10.1128/AAC.00893-09
852 86. Sanz-garcía F, Hernando-amado S, Martínez L. Mutation-Driven Evolution of
853 Pseudomonas aeruginosa in the Presence of either Ceftazidime or
854 Ceftazidime-Avibactam. Antimicrob Agents Chemother. 2018;62: e01379-18.
855 87. Winsor GL, Griffiths EJ, Lo R, Dhillon BK, Shay JA, Brinkman FSL. Enhanced
856 annotations and features for comparing thousands of Pseudomonas genomes
857 in the Pseudomonas genome database. Nucleic Acids Res. 2015;44: D646–
858 D653. doi:10.1093/nar/gkv1227
859 88. Kahm M, Hasenbrink G, Ludwig J. grofit: Fitting Biological Growth Curves with
860 R. J Stat Softw. 2010;33: 1–21. doi:10.18637/jss.v033.i07
861

862 **Figures**

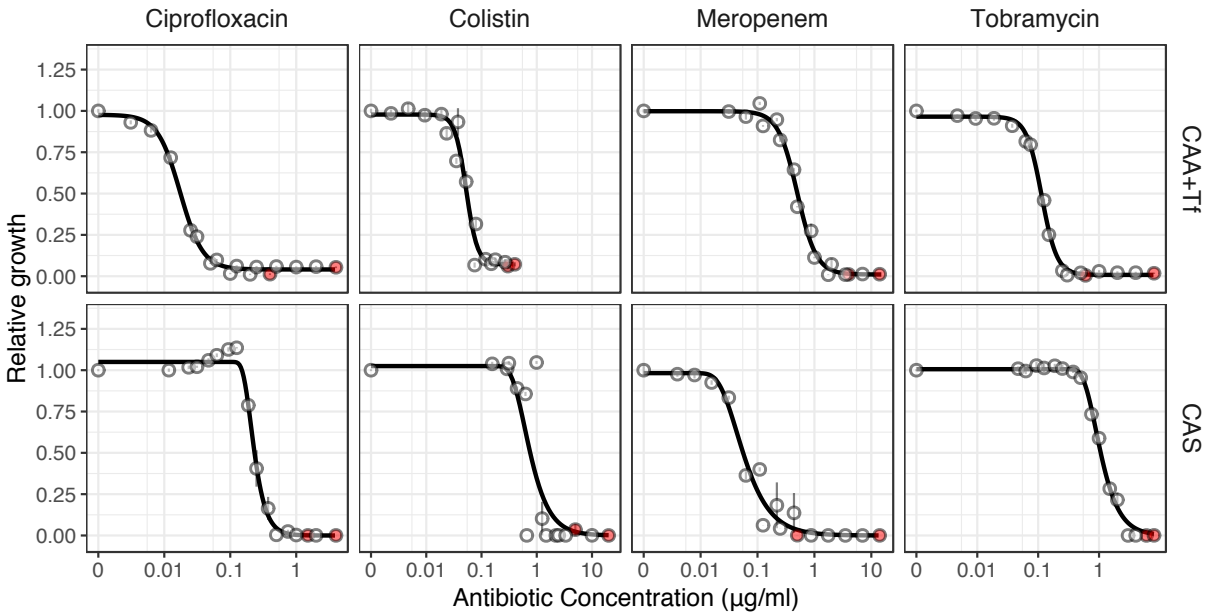

863

864 **Figure 1. Antibiotic dose response curves for *P. aeruginosa* PAO1 populations**.
865 We exposed PAO1 to all four antibiotics in two experimental media: CAA+Tf (iron-
866 limited casamino acids medium with transferrin) and CAS (casein medium). Except for
867 meropenem, higher concentrations of antibiotics were required to inhibit PAO1 in CAS
868 compared to CAA+Tf. Dots show means ± standard error across six replicates. All
869 data are scaled relative to the drug-free treatment. Data stem from two independent
870 experiments using different dilution series. The red dots indicate the highest
871 concentration used for the respective experiments, from which 7-serial dilution steps
872 were tested. Curves were fitted with either log-logistic functions (in CAA+Tf) or with
873 three-parameter Weibull functions (in CAS).

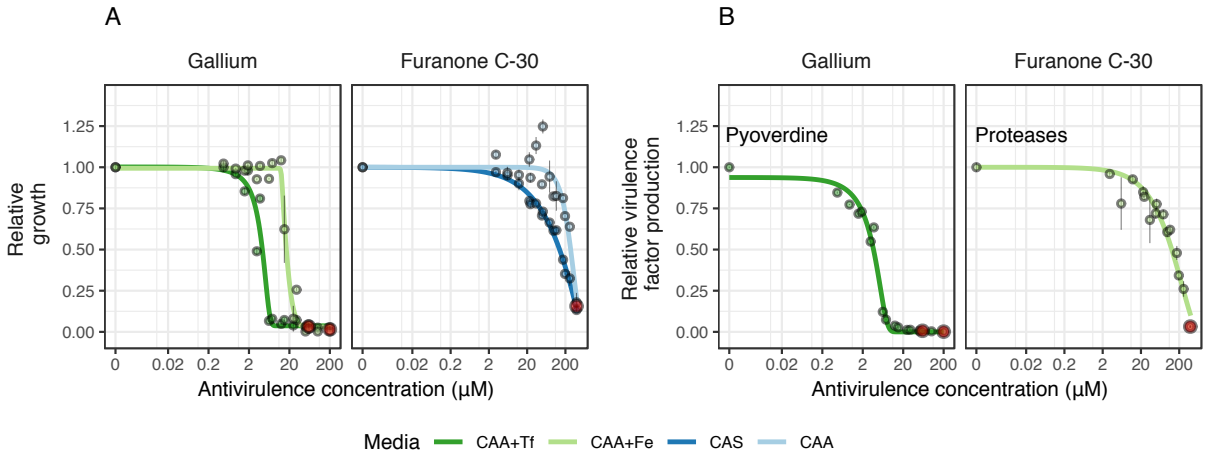

874

875 **Figure 2. Antivirulence dose response curves for *P. aeruginosa* PAO1**
876 **populations (growth and virulence factor production)**. We exposed PAO1 to the
877 antivirulence compounds gallium (inhibiting pyoverdine-mediated iron uptake) and
878 furanone C-30 (blocking quorum sensing response including protease production) both
879 in media where the targeted virulence factors are expressed and required (iron-limited
880 CAA+Tf medium for gallium and CAS medium for furanone) and in control media
881 where the targeted virulence factors are not required (iron-supplemented CAA+Fe
882 medium for gallium and protein digested CAA for furanone). (**A**) Dose-response curves
883 for growth show that both antivirulence compounds reduced bacterial growth, but more
884 so in media where the targeted virulence factor is expressed. This demonstrates that
885 there is a concentration window where the antivirulence compounds have no toxic
886 effects on bacterial cells and just limit growth due to virulence factor quenching. (**B**)
887 Dose-response curves for virulence factor production show that gallium and furanone
888 C-30 effectively inhibit pyoverdine and protease production, respectively, in a
889 concentration-dependent manner. Dots show means ± standard errors across six
890 replicates. All data are scaled relative to the drug-free treatment. Data stem from two
891 independent experiments using different dilution series. The red dots indicate the
892 highest concentration used for the respective experiments, from which 7-serial dilution
893 steps were tested. Curves were fitted with either log-logistic functions (in CAA+Tf) or
894 with three-parameter Weibull functions (in CAS).

895

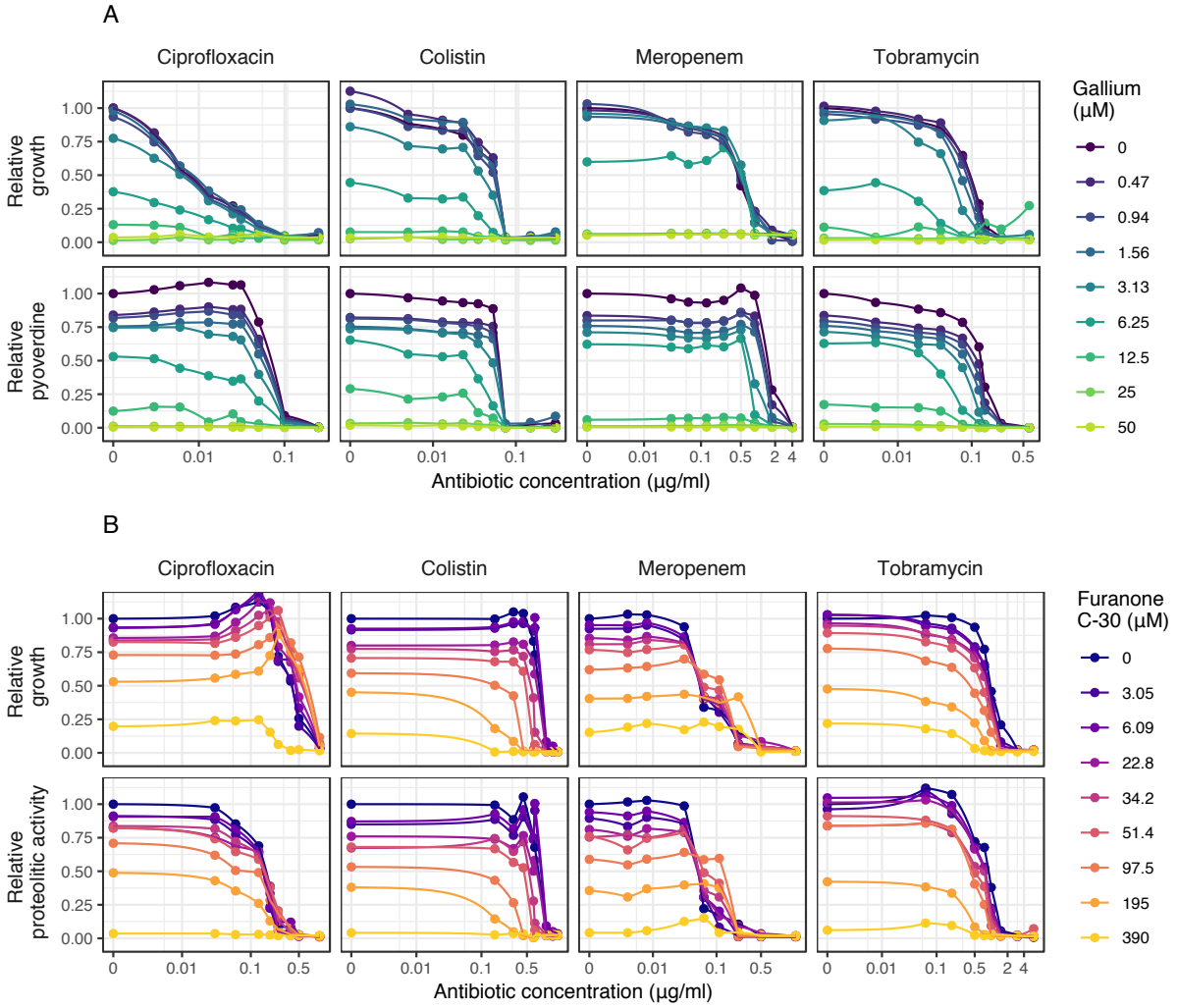

Figure 3. Dose response curves for *P. aeruginosa* PAO1 populations under antibiotic-antivirulence combination treatments. Dose-response curves for growth and virulence factor production for PAO1 were assessed for 9x9 drug concentration matrixes involving the four antibiotics combined with either gallium (**A**) or furanone C-30 (**B**). Experiments were carried out in media where the corresponding virulence factors are required for growth (pyoverdine: CAA+Tf; protease: CAS). Growth and virulence factor production were measured after 48 hours. All values are scaled relative to the untreated control, and data points show the mean across 12 replicates from two independent experiments. We used spline functions to fit the dose-response curves.

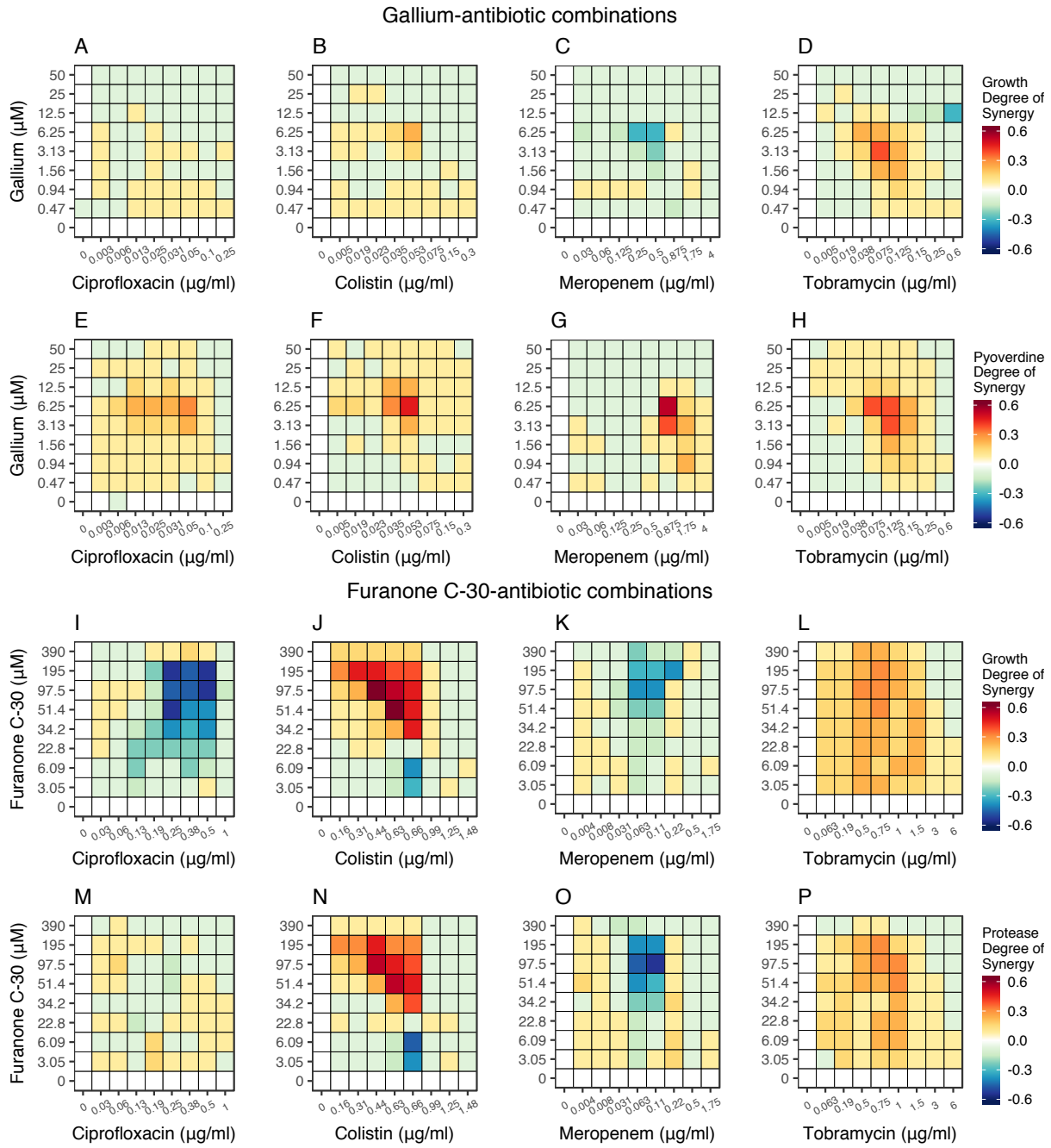

Figure 4: Drug interaction heatmaps for antibiotic-antivirulence combination treatments. We used the Bliss independence model to calculate the degree of synergy for every single drug combination with regard to growth suppression and virulence factor quenching shown in Figure 3. Heatmaps, depicting variation in drug interactions ranging from antagonism (blue) to synergy (red), are shown for gallium-antibiotic combinations (**A-D** for growth; **E-H** for pyoverdine production) and furanone-antibiotic combinations (**I-L** for growth; **M-P** for protease production). All calculations are based on 12 replicates from two independent experiments.

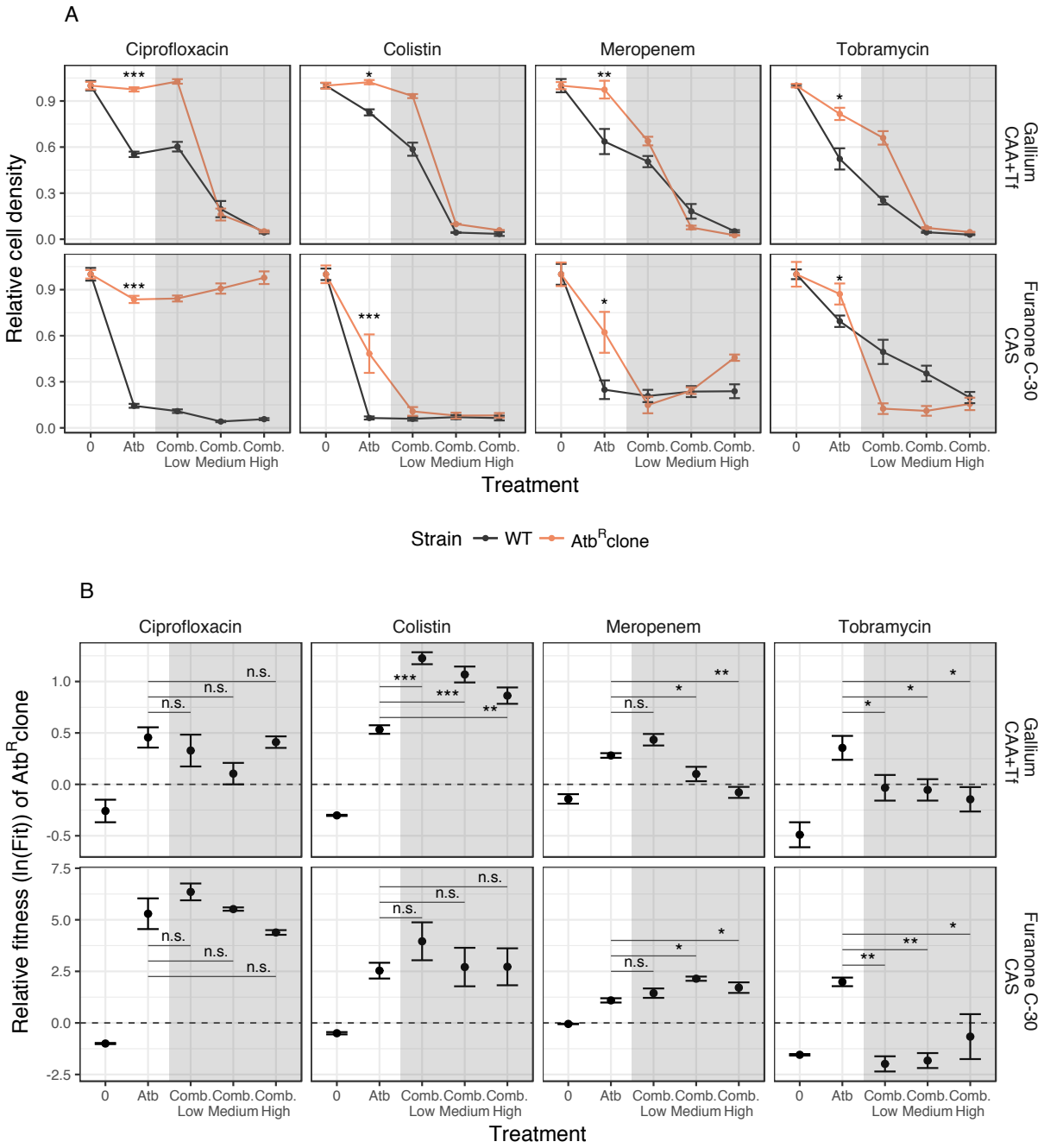

Figure 5: Effect of combination treatment on the fitness of antibiotic resistant clones. (**A**) Test of whether the addition of antivirulence compounds can restore growth suppression in antibiotic resistant clones (AtbR, in orange) relative to the susceptible wildtype (WT, in black). Under antibiotic treatment and in the absence of antivirulence compounds, all AtbR strains grow significantly better than the WT, a result that holds for both scaled (as shown above) and absolute growth. In the presence of antivirulence compounds (gray shaded area), growth suppression was restored in seven out of eight drug combinations (except for the furanone-ciprofloxacin combo). Antivirulence compound concentrations used for gallium: 1.56 μM (combo

928 low), 6.25 μM (combo medium), 12.5 μM (combo high); for furanone C-30: 6.1 μM
929 (combo low), 22.8 μM (combo medium), 51.4 μM (combo high). Important to note is
930 that all antivirulence compound concentrations do not or only mildly affect pathogen
931 growth when applied as single treatments (Figure 2). All cell density values (measured
932 with flow cytometry as number of events detected in 5 μl of culture, after 24 hours) are
933 scaled relative to the untreated control. (**B**) Test of whether the addition of
934 antivirulence compounds can revert selection for antibiotic resistance during
935 competition between AtbR and WT, starting at a 1:9 ratio. The dashed lines denote
936 fitness parity, where none of the competing strains has a fitness advantage. With no
937 treatment, all AtbR strains showed a fitness disadvantage (fitness values < 0)
938 compared to the WT. When treated with antibiotics alone, all AtbR strains experienced
939 significant fitness advantages. When antivirulence compounds were added as
940 adjuvants, this fitness advantage was lost for three drug combinations: meropenem-
941 gallium, tobramycin-gallium, tobramycin-furanone C-30, thus showing reversal of AtbR
942 selection. All data are shown as means ± standard errors across a minimum of eight
943 replicates from two to three independent experiments. Significance levels are based
944 on ANOVAs: n.s. = non-significant; * $p < 0.05$; ** $p < 0.01$; *** $p < 0.001$. See
945 Supplementary Table S3 for details on statistical analysis.

946 **Table 1. List of mutations in the antibiotic resistant clones**

AtbR clone[a,b]	Combination with	Gene[c]	Description	Mutation type[b]	Reference	Variant	Position[d]	Reference
CpR_1	Gallium Furanone C-30	*gyrB*	DNA gyrase subunit B	INDEL	CCCAGGAG	CG	5671	[36]
		mexR	Multidrug resistance operon repressor	INDEL	ATCAGTGCCT TGTCGCGGCA	AA	471547	[37,82]
CoR_1	Gallium	*phoQ*	Two-component sensor PhoQ	SNP	T	G	1279140	[38,83–85]
CoR_2	Furanone C-30	*phoQ*	Two-component sensor PhoQ	INDEL	T	TC	1279085	[38,83–85]
				SNP	T	C	1279089	
		PA1327	Probable protease	INDEL	CA	C	1440622	
MeR_1	Gallium	*mpl*	UDP-N-acetylmuramate:L-alanyl-gamma-D-glutamyl-meso-diaminopimelate ligase	SNP	T	G	4499740	[39,86]
MeR_2	Furanone C-30	*parR*	Two-component response regulator, ParR	SNP	C	T	1952257	[40]
		PA1874	Hypothetical protein (efflux pump)	COMPLEX	ACCGGG	CCCGTC	2039326	[41]
				SNP	A	G	2039485	
				SNP	C	T	2039494	
				SNP	T	C	2039512	
				SNP	G	A	2039517	
				SNP	T	C	2039524	

				COMPLEX	CGGG	TGGC	2039530	
		nalD	Transcriptional regulator NalD	SNP	A	C	4006981	[42,43]
TbR_1	Gallium	*fusA1*	Elongation factor G	SNP	C	T	4769121	[44]
				SNP	T	G	5253694	
TbR_2	Furanone C-30	*fusA1*	Elongation factor G	SNP	T	C	4770785	[44]
		pscP	Translocation protein in type III secretion system	INDEL	$TG(TTGGCG)_{x11}$	$TG(TTGGCG)_{x12}$	1844903	
		PA4132	Conserved hypothetical protein	SNP	A	C	4621443	

[a]The antibiotic resistant strains are referred to as AtbR throughout the text.

[b]Abbreviations: Atb: antibiotic; Cp: ciprofloxacin; Co: colistin; Me: meropenem; Tb: tobramycin; SNP: single nucleotide polymorphism; INDEL: insertion or deletion; COMPLEX: multiple consecutive SNPs .

[c]Mutations in the ancestor wildtype background compared to the reference PAO1 genome are reported in [73].

[d]Position on PAO1 reference genome [87].